Paracrine secretion of MUFAs prevents ferroptosis in triple-negative breast cancer and reveals selenocysteine synthesis dependency for lung metastasis

Tobias Ackermann[1], Engy Shokry[1], Ruhi Deshmukh[1], Jayanthi Anand[1], Laura C.A. Galbraith[1], Louise Mitchell[1], Giovanny Rodriguez-Blanco[1], Victor H. Villar[1], Britt Amber Sterken[1], Colin Nixon[1], Sara Zanivan[1,2], Karen Blyth[1,2], David Sumpton[1] and Saverio Tardito[1,2]

[1]Cancer Research UK Beatson Institute; Garscube Estate, Switchback Road, Glasgow, G61 1BD, UK.

[2]School of Cancer Sciences, University of Glasgow; Glasgow, G611QH, UK.

Abstract

The limited availability of therapeutic options for patients with triple-negative breast cancer (TNBC) contributes to the high rate of metastatic recurrence and poor prognosis. Ferroptosis is a type of cell death caused by iron-dependent lipid peroxidation counteracted by the antioxidant activity of selenoproteins. Here, we show that TNBC cells secrete an anti-ferroptotic factor in the extracellular environment when cultured at high cell densities but are primed to ferroptosis when forming colonies from single cells. We found that secretion of the anti-ferroptotic factor, identified as monounsaturated fatty acid (MUFA) containing lipids, and the vulnerability to ferroptosis of single cells depends on the expression of stearyl-CoA desaturase (SCD) that is proportional to cell density. Finally, we show that the inhibition of tRNAsec selenocysteinilation, an essential step for selenoprotein production, causes ferroptosis and impairs the lung seeding of circulating TNBC cells that are no longer protected by the MUFA-rich environment of the primary tumour.

Introduction

Ferroptosis is a form of cell death caused by iron-dependent peroxidation of polyunsaturated fatty acids (PUFA) within membranes. Peroxidised lipids cause stiffening and thinning of the membrane bilayer making it prone to rupture [1,2]. In recent years, several cell-intrinsic pathways that prevent or revert lipid peroxidation have been discovered. To reduce lipid peroxides, cells rely on lipophilic antioxidants such as tetrahydrobiopterin, ubiquinone, vitamin K and E, and membrane-associated peroxidases like the selenoprotein GPX4 [3–5]. In addition, the fatty acid composition of the membrane influences the cellular susceptibility to ferroptosis. The synthesis of saturated fatty acids and the Acyl-CoA Synthetase Long Chain Family Member 4 (ACSL4) mediated incorporation of PUFAs into membranes promote ferroptosis [6,7]. On the other hand, membrane incorporation of the exogenously supplemented monounsaturated fatty

acid (MUFA) oleic acid, as well as its cell-autonomous production mediated by the stearoyl-CoA desaturase (SCD), has been shown to prevent ferroptosis *in vitro* and *vivo* [8–10] .

Selenocysteine is a genetically encoded amino acid that incorporates a selenium atom. Proteins that incorporate selenocysteine are defined as selenoproteins. During mRNA translation, selenocysteine is incorporated by a recoding event. If an mRNA contains a selenocysteine insertion sequence (SECIS), the canonical UGA stop codon is translated to selenocysteine. In addition, selenocysteine incorporation into peptides depends on the presence of specific translation factors, the eukaryotic elongation factor selenocysteine (eEFsec) and SECIS binding protein (SECISBP2) [11]. Despite the chemical similarity, cysteine and selenocysteine do not share the biosynthetic pathway. Indeed, selenocysteine is synthesised on the selenocysteine tRNA ($tRNA^{sec}$) that is firstly charged with serine by seril-tRNA synthetase. The serine on the $tRNA^{sec}$ is then phosphorylated by phosphoseryl-tRNA kinase (PSTK). The selenophosphate ($SePO_3^{(3-)}$) synthesized by the Selenophosphate Synthetase 2 (SEPHS2) is used by O-phosphoseryl-$tRNA^{Sec}$ selenium transferase (SEPSECS) to synthesize selenocysteinilated $tRNA^{sec}$. This is the only known pathway to produce the selenocysteinilated $tRNA^{sec}$ and free selenocysteine obtained from selenoproteins degradation cannot be directly charged on $tRNA^{sec}$ [12].

The supplementation with an excess of selenium and the inhibition of $tRNA^{sec}$ synthesis can both lead to the accumulation of reactive selenium species toxic to cancer cells [13,14]. On the other hand, selenium deprivation has been shown to induce ferroptosis in cells from breast cancer, acute myeloid leukaemia, and neuroblastoma [15–17]. Several pre-clinical and clinical studies assessed selenium supplementation as an antioxidant cancer-preventive intervention and selenium is frequently found in fortified food, and multivitamin/multimineral supplements [18,19].

However, susceptibility to ferroptosis does not only depend on selenium availability. In this study, we show that triple-negative breast cancer (TNBC) cells under selenium starvation or GPX4 inhibition die of ferroptosis selectively when seeded at low density. We found that this phenotype can be rescued by transferring medium conditioned by high density cultures of breast cancer cells or cancer associated fibroblasts but not normal cells. By means of analytical methods coupled with mass spectrometry-based lipidomics we identified SCD-derived MUFA-containing lipids as the anti-ferroptotic factors released by TNBC cells. Finally, we interfered with the expression of genes of the selenocysteine biosynthesis pathway to prove that *in vivo* TNBC cells requires the antioxidant action of selenoproteins to overcome the pro-ferroptotic environment encountered during the metastatic cascade.

Materials and Methods

Cell culture

Cultures of breast cancer cells (BT549, Cal120, EO771, MCF7, MDA-MB-231 and MDA-MB-468), human dermal fibroblast (DF), human mammary fibroblast (MF) and cancer associated fibroblast (CAF) were maintained in DMEM/F-12 (Thermo Fisher Scientific, #21331046) supplemented with 2 mM Glutamine (Thermo Fisher Scientific, #25030149) and 10% foetal bovine serum (FBS, Thermo Fisher Scientific, #10270106). MF and CAF cell lines were kindly provided by Prof. Akira Orimo and have been previously characterised [20,21]. All cell lines were tested negative for mycoplasma (Venor GeM qOneStep Mycoplasma Detection Kit).

Conditioned medium

To condition medium from high density cultures of BT549, Cal120, EO771, MCF7, MDA-MB-231, MDA-MB-468, DF, MF and CAF cell lines, $6x10^6$ cells were seeded in DMEM/F-12 with 10% FBS in a dish with a diameter of 145mm. The day after seeding, the medium was replaced with 20 ml of DMEM/F-12 without FBS and conditioned for two days. For non-targeting control (NTC) and SCDko MDA-MB-468 cells, $5x10^6$ and $1.1x10^7$ cells were seeded respectively to condition the medium. For experiments with acute SCD inhibition, $2x10^7$ MDA-MB-468 cells were seeded in DMEM/F-12 with 10% FBS. The day after seeding the medium was replaced by DMEM/F-12 without FBS and supplemented with 200 nM CAY10566 (SCD inhibitor, Cayman chemicals, #10012562). After 18h incubation with 200 nM CAY10566, cells were washed once with PBS, and 15 ml DMEM/F-12 medium without FBS was conditioned for 2h.

To generate mock medium, cell culture medium was incubated in a cell culture dish maintained at 37°C without cells for the respective experimental time periods (2h or 2 days).

Colony formation assays

Colony formation assays were performed as descripted previously [16]. For MDA-MB-468 cells, we seeded 5,000 cells/well in a 6 well plate with 2 ml/well of DMEM/F-12 supplemented with 2.5% FBS. To test the effects of lipid extracts from medium conditioned by MDA-MD-468 cells, 1,000 cells/well were seeded in a 24 well plate with 0.5ml of medium/ well. After 7 days incubation, colonies from MDA-MB-468 cells were fixed by replacing the medium with a solution of 3% trichloroacetic acid in water (Merck, #T6399-500G), rinsed twice with water, stained with 0.057% Sulforhodamine B solution (in 1% acetic acid, Merck, #230162) and washed twice with a 1% acetic acid solution in water. For BT549, Cal120, MCF7, MDA-MB-231 and EO771 cells, 500 cells/well were seeded in a 6 well plate and fixed after 14 days of culture with the exception of EO771 cells that were fixed 7 days after seeding. Plates stained

with Sulforhodamine B were scanned with Li-Cor Odyssey® DLx imaging system and the fluorescent signal quantified with ImageJ as previously described [16].

Cell proliferation assay

To determine the number of NTC control and SCDko cells during the medium conditioning experiments, $3.32x10^5$ NTC control cells per well and $7.3x10^5$ SCDko cells per well were seeded in a 6 well plate with DMEM/F-12 containing 10% FBS. One day after seeding, cells were trypsinized and counted with Casy counter. At this time, the medium was replaced with DMEM/F-12 without FBS in a second plate seeded and incubated in the same conditions, and two days after cells were counted with a Casy counter.

For proliferation assays, NTC control or SCDko MDA-MB-468 cells were seeded at $3x10^4$/ well in a 6 well plate with DMEM/F-12 supplemented with 2.5% FBS, 50 nM Na_2SeO_3 (Merck, #S5261), 1 µM Ferrostatin-1 (Merck, #SML0583) or 10 µM oleic acid (Merck, #O1008) or vehicles (0.05% DMSO and 0.02% ethanol). For proliferation assays with GPX4 inhibitor (RSL3), cells were seeded and incubated as described above and supplemented with 50 nM RSL3 (Merck, #SML2234) and 10% FBS. After 5 days, cells were counted with a Casy counter or stained with Sulforhodamine B and images acquired and analysed as described for the colony formation assays.

Medium fractionation and heat inactivation

Medium conditioned by MDA-MB-468 cells was loaded into size exclusion columns (Amicon® Ultra-15 Ultracel-10 Centrifugal Filter Unit, Merck, #UFC901024) centrifuged at 4,000g for 30 min and the fractions stored at -20ºC until further analysis. The concentrated fraction (CM>10kDa) was diluted 1:40 in unconditioned DMEM/F-12 medium, supplemented with 2.5% FBS and used for a colony forming assay. The column flow-through (CM<10kDa) was supplemented with 2.5% FBS and used undiluted for a colony forming assay.

For heat inactivation and protein denaturation, the concentrated fraction (CM>10kDa) was incubated for 15 min at 95ºC, afterwards diluted 1:40 in unconditioned DMEM/F-12 medium supplemented with 2.5% FBS and used for a colony forming assay.

Lipid extraction

Lipids were extracted following the Bligh and Dyer method or with a methyl tertiary-butyl ether (MTBE) solution. For the Bligh and Dyer extraction, 250 µl of the concentrated fraction (CM>10kDa) from the size exclusion columns were mixed with 960 µl of a 1:2 chloroform:methanol mixture. Afterwards, 310 µl chloroform and 310 µl water were added and the solution mixed to achieve a phase separation. The lower, chloroform containing phase

was transferred to a new glass vial, dried at room temperature by nitrogen flow and resuspended in 25 µl of ethanol. 5 µl of lipid containing ethanol was supplemented to 2 ml of DMEM/F-12 with 2.5% FBS to perform colony forming assays.

For the MTBE extraction, 5 ml MTBE and 1 ml methanol were added to 2.5 ml of conditioned medium. After mixing the solution three times for 30 s, the upper phase was transferred to a new glass vial, dried under nitrogen flow at 35ºC and resuspended in 25µl ethanol. 1 µl of the lipid ethanol solution was supplemented to 1 ml of DMEM/F-12 with 2.5% FBS and used for a colony forming assay.

Lipidomic analysis

For lipidomic analysis, $5x10^5$ NTC control and SCDko cells were seeded in 20 ml of DMEM/F-12 supplemented with 2.5% FBS in plates of 145 mm diameter. After 2 days, cells were scraped off the plate in the culture medium, collected in a tube and centrifuged at 1,000g for 3 min. The cell pellet was resuspended in 1 ml of ice-cold PBS, transferred to 1.5 ml 5Eppendorf vial, and centrifuged at 10,000 g for 10 s. Lipids were extracted from the cell pellet with 200 µl of butanol:methanol solution (1:1) centrifuged at 16,000g for 10 minutes, and analysed using high resolution mass spectrometry.

For the lipidomic analysis of media 10 µl of conditioned medium enriched (CM>10kDa) or depleted (CM<10kDa) fractions were diluted with 190 µl of butanol:methanol solution (1:1), centrifuged at 16,000g for 10 minutes, and analysed using high resolution mass spectrometry.

Lipidomic analyses were performed using a Thermo Fisher Scientific Ultimate 3000 binary UPLC coupled to a Q Exactive Orbitrap mass spectrometer equipped with a Heated Electrospray Ionization (HESI-II) source (Thermo Fisher Scientific, Massachusetts, USA). For each sample, MS data were acquired using full MS/ dd-MS2 in positive and negative modes to maximize the number of detectable species. Details on the parameters for the MS methods using different polarities is provided in Table 1.

Chromatographic separation was achieved using a Waters CSH C18 analytical column (100 x 2.1mm, 1.7µm) maintained at 55ºC. The mobile phase consisted of 60:40 (v/v) acetonitrile:water containing 10 mM ammonium formate and 0.1% formic acid (phase A) and 90:10 (v/v) isopropanol:acetonitrile containing containing 10 mM ammonium formate and 0.1% formic acid at a flow rate of 400 µl/min. The gradient elution consisted of 30% B for 0.5 min, which increases linearly to reach 50% at 4 min, then 80% at 12 min, then 99% A at 12.1 min then held at 99% for 1 min, then returned back to starting condition in 1 min and kept constant for 2 min. The total run time was 20 min. The whole system was controlled by Xcalibur version

4.3. Quality control (QC) samples prepared by mixing equal volumes of experimental samples were injected at regular interval throughout the whole batch to monitor the instrument performance. Lipidomics data were analysed with Compound Discoverer v.3.1 (ThermoFisher Scientific) and LipiDex, an open-source software suite available at http://www.ncqbcs.com/resources/software/. Briefly, raw files were loaded into Compound Discoverer and processed using two workflows (aligned and unaligned) as previously described [22]. Compound result tables were exported for further processing using the 'Peak picking' tab in Lipidex. In addition, the raw data files were converted to .mgf files using MSConvert (ProteoWizard, P. Mallick, Stanford University) and imported into the 'Spectrum Searcher' tab in Lipidex, where the following libraries were searched 'LipidBlast_Formate', 'LipiDex_HCD_Formate', 'LipiDex_Splash_ISTD_Formate', 'LipiDex_HCD_ULCFA' using the default search tolerances for MS1 and MS2. For a lipid to be considered identified it required a minimum of 75% spectral purity, an MS2 search dot product score of at least 500 and reverse dot product of at least 700. Z scores were calculated in Perseus version 1.6.2.2 and used for the heatmap reported in Figure 3.

For the determination of the total fatty acid content of the lipid species, samples were analysed using GC-MS after transesterification using a methanolic solution of (m-trifluoromethylphenyl) trimethyl ammonium hydroxide (Meth-Prep II), to provide fatty acid methyl esters (FAME) in a one-step reaction followed by monitoring of the generated FAME using GC/MS in SIM mode. Briefly, samples were first spiked with heptadecanoic (C17:0) as an internal standard, dried under nitrogen stream and resuspended in 27µL of chloroform. 3 µL of Meth-Prep II were added and samples were mixed and analysed within 2 days. Analysis was performed using an Agilent 7890 GC chromatograph and 7693 autosampler coupled with an Agilent 7000 GC/MS provided with (Agilent, CA, United states). High purity helium (99.999%) was used as carrier gas at an initial flow rate of 1 mL/min increased to 2 mL/min in 12 seconds and kept constant for 1 min and then returned to 1mL/min for the rest of the run time. The chromatographic column used was Phenomen BPX70 (60 m x 250 µm, 0.25 µm) (Fisher Scientific, USA). The injector was set at a temperature of 300 °C, a pressure of 21 psi and a septum purge flow of 3mL/min. Injection was performed in a pulsed splitless mode at 60 psi for 1.2 min and a purge flow to split vent of 50 mL/min at 1.2 min. The injection volume was 1 µl. The oven temperature was set to an initial temperature of 100°C held for 2 min followed by a linear increase to 172°C at 8°C/min (held for 6 min), then 196°C (held for 9 min) then 204°C (held for 15 min). The total run time was 45 minutes. The MS was operated in electron ionization (EI) mode at 70 eV and the MSD transfer line was set to 260 °C. MS data were acquired in SIM mode for monitoring of the individual fatty acid derivatives. MS recording started at a cut-off of 8 min. Data were processes using Agilent MassHunter Quantitative

analysis software (Agilent, CA, United states). Initially, fatty acids were annotated by comparison to FAME Standard Mixture (Merck Life Science UK Limited, United Kingdom) using a combination of retention time and fragmentation pattern using full scan. A SIM mode for selected fragments was applied to improve the sensitivity of detection.

Table 1. Parameters of the mass spectrometry methods using positive and negative polarities.

Parameters	Positive Mode	Negative Mode
Source parameters:		
- Capillary Temperature:	262.5ºC	300.0 ºC
- Sheath gas:	50.0	50.0
- Aux gas:	12.5	7.0
- Spare gas:	2.5	5.0
- Probe heater Temperature:	425.0 ºC	300.0 ºC
- S-Lens RF level:	50	50
Full MS:		
- Chromatographic peak width	15s	10s
- Default Charge:	1	1
- Resolution:	70,000	70,000
- AGC target:	3e6	3e6
- Maximum IT:	100ms	100ms
- Scan range:	240-1200 m/z	240-1600 m/z
dd-MS2:		
- Resolution:	17,500	17,500
- AGC target:	2e5	1e5
- Loop count:	5	5
- Isolation window:	1.4 m/z	1.4 m/z
- Stepped nce:	25	25
- Spectrum data:	centroid	centroid
dd-settings:		
- Minimum AGC:	4e3	1e3
- Exclude Isotopes:	On	On
- Dynamic exclusion:	8s	5s

Cloning and CRISPR-based gene editing

The following gRNA sequences: Non Targeting Control (NTC): 5'-GTAGCGAACGTGTCCGGCGT-3', *PSTK*: 5'-AAACTGATCAGACACTCCGA-3', *SCD*: 5'-GCAGCCGAGCTTTGTAAGAG-3', *SEPHS2*: 5'-GAGGGACGGCAGTGACCGG-3', *SEPSECS*: 5'-AACCGCGAGAGCTTCGCGG-3' were cloned into lentiCRISPRv2 vector (Addgene, Plasmid #52961) using BsmBI restriction sites. For lentivirus production, $2x10^6$ HEK293T cells were transfected with 5 µg lentiCRISPR plasmid (NTC or on target), 1µg pVSV-G (viral envelope) and psPAX2 (2nd generation lentiviral packaging plasmid) using JetPrime (Polyplus, #101000015) according to the manufacturer's protocol. Six hours after

transfection the medium was replaced, incubated for 18 hours and harvested for viral infection of recipient cells. The recipient MDA-MB-468 cells were cultured for 24 hours with lentivirus-containing medium supplemented with 8 µg/ml Polybrene, for an additional 24 hours with fresh medium and selected for 4 days with medium supplemented with 0.75µg/mL puromycin.

After infection, SCD ko pools and clones were cultured in DMEM/F-12 with 10% FBS and 0.8 g/L AlbuMAX II lipid-rich BSA (Thermo Fisher Scientific, # 11021029). sgPSTK, sgSEPHS2 and sgSEPSECS cell lines were cultured in DMEM/F-12 with 2.5% FBS, 0.8 g/l AlbuMAX II lipid-rich BSA and 1µM Ferrostatin-1 (MERCK, # SML0583-5MG) unless otherwise indicated.

Firefly luciferase expression cassette (fluc+) was excised from pGL4.50 vector (Promega, # E1310) using NdeI and BamHI restriction enzymes and cloned into pLenti6NEO vector using the same restriction sites. The integration of the cloned fragment was confirmed by sanger sequencing. Virus production and infection of MDA-MB-468 target cells was performed as described above for lentiCRISPR vectors. After the infection cells were selected for 7 days with 500 µg/ml G-418S sulphate (Formedium, # G418S). Luciferase activity was checked by supplementing the culture medium with luciferin (100 µg/ml, Abcam, #ab143655) and the bioluminescent signal assessed with a Tecan Spark multiplate reader.

Lipids peroxidation assay

$5x10^5$ NTC control and SCDko cells were seeded in DMEM/F-12 supplemented with 2.5% FBS in plates of 145mm diameter. 2 days after seeding cells were incubated for 30 minutes with 1 µM BODIPY 581/591 C11 lipid peroxidation sensor (Thermo Fisher Scientific, #D3861). Cells were then washed with PBS, detached by trypsinisation, pelleted by centrifugation and resuspended in 400 µL PBS with 1 µg/ml DAPI used to stain dead cells. Peroxidation of the BODIPY probe in live cells was measured by fluorescent-activated flow cytometry (FACS). The fluorescence of the reduced probe was measured at 581/591 nm (excitation/emission, Texas Red filter set) and the oxidised probe at 488/510 nm (FITC filter set). The ratio between the signals at 510 and 591 nm (oxidised/reduced) was used as a readout for lipid peroxidation. $5x10^5$ NTC control and SCDko cells exposed to 100 nM RSL3 for 2 hours were used as positive control for lipid peroxidation.

Immunoblotting

Cells were lysed in radioimmunoprecipitation assay (RIPA) buffer (Millipore, #20-188). Lysates were incubated in Laemmli buffer (Bio-rad, #1610747) at 95ºC for 3 min and loaded onto a SDS-polyacrylamide gel (4-12%, Invitrogen NuPAGE, #NP0336BOX). After size separation, proteins were transferred onto nitrocellulose membrane (0.2 µM pore size, Amersham, #

10600001) and membrane was blocked for 1h at room temperature by 5% non-fat dry milk (in tris-buffered saline with 0.01% Tween (TBST)). Membranes were incubated overnight at 4ºC in a 5% BSA/TBST solution of primary antibody at the following dilutions: vinculin, 1:2000, Merck, # SAB4200080; GPX4, 1:1000, Abcam, # ab125066; SCD, 1:1000, Alpha Diagnostics, #SCD11-A; SEPHS2, 1:1000, Merck, # SAB2700271. The next day membranes were washed and stained with species-specific near-infrared fluorescent, secondary antibodies (Li-COR) for 1h at room temperature. After additional washing steps, membranes were imaged with Li-Cor Odyssey® DLx imaging system.

RNA isolation and qRT-PCR analysis

The same number of MDA-MB-468 cells (1.6 $x10^5$) were seeded per well in a 6 well plate or in plates of 145mm diameter for high- and low-density cultures, respectively. For BT549, CAL120, MDA-MB-231 and MCF7 cells, low- and high-density cultures were achieved by seeding $4x10^4$ cells in plates of 145mm diameter and $1.6x10^5$ per well in a 6 well plate, respectively. 2 days after seeding, the cells were washed with ice-cold PBS, scraped off the plate and pelleted at 4ºC at 10,000g for 30s. RNA was isolated from cell pellets and tumour fragments following the kit manufacturer's protocol (Qiagen RNeasy, # 74104). 500 ng RNA was used for cDNA synthesis (SuperScript VILO MasterMix, # 11755-050). 5ng cDNA and 8 pmol of each primer were used in each quantitative real-time polymerase chain reaction (Applied Biosystems Fast SYBR Green Master Mix, #4385612). Primer sequences were obtained from primer bank (https://pga.mgh.harvard.edu/primerbank/). A standard curve method with linear regressions R^2> 0.8 was used to obtain relative quantification of mRNAs expression.

Gene symbol	forward primer (5'-3')	reverse primer (5'-3')
ACACA	TCACACCTGAAGACCTTAAAGCC	AGCCCACACTGCTTGTACTG
ACTB	GGCATGGGTCAGAAGGATT	ACATGATCTGGGTCATCTTCTC
ELOVL3	CTGTTCCAGCCCTATAACTTCG	GAATGAGGTTGCCCAATACTCC
FADS1	CTACCCCGCGCTACTTCAC	CGGTCGATCACTAGCCACC
FADS2	GACCACGGCAAGAACTCAAAG	GAGGGTAGGAATCCAGCCATT
FASN	AAGGACCTGTCTAGGTTTGATGC	TGGCTTCATAGGTGACTTCCA
SCD	TCTAGCTCCTATACCACCACCA	TCGTCTCCAACTTATCTCCTCC
SEPHS2	GCGGCTGAGGAAGGAGGGACG	ACGGCGCTGTCCGGCATTATG

Xenograft experiments

Animal experiments were performed in accordance with UK Home Office Regulations and Directive 2010/63/EU, and subjected to review by the Animal Welfare and Ethical Review

Board of the University of Glasgow (Project licence PP6345023 and P38F4A67E). In house-bred NOD SCID gamma (NSG) mice were housed at temperatures between 19 and 23 ºC in ventilated cages with *ad libitum* food and water access and 12 hours light/dark cycles. 24 hours before xenotransplantation Rimadyl was added to the drinking water and removed 3 days after implantation. Six female NSG mice of 94 days of age were anesthetized and injected into the inguinal mammary fat pad with 50 µl per injection of 1:1 PBS:Matrigel solution containing $3x10^6$ luciferase-expressing MDA-MB-468 cells. Three animals were randomly assigned to each of the two experimental groups (NTC and sgSEPHS2). All the mice were injected bilaterally, with the exception of one mouse of the NTC group that was injected unilaterally due to a technical issue. Tumours were measured by calliper 3 times/week by animal technicians blinded to the scientific outcome. The tumour volume was calculated using the equation ([length × $width^2$]/2, where width is the smaller of the two values). 35 days post-transplant mice were culled, and mammary tumours, lungs and livers were harvested. Lungs and livers were checked for metastasis *ex vivo* by IVIS Spectrum imaging system (PerkinElmer). Tissues were fixed in 10% buffered formalin solution and embedded in paraffin.

To assess the metastatic seeding capacity of breast cancer cells, $2x10^6$ luciferase expressing MDA-MB-468 cells were strained (70 µm), resuspended in 100µL of 4.5% BSA PBS solution (pH 7.4), and injected into the tail vein of six female NSG mice of 55-146 days of age. Three aged-matched animals were assigned to each of the two experimental groups (NTC and sgSEPHS2). Mice were imaged weekly by IVIS and culled 7-weeks after injection prior to reaching clinical endpoint. Organs were harvested, fixed in 10% buffered formalin solution and embedded in paraffin for immunohistochemistry.

Immunohistochemistry

All immunohistochemistry (IHC) staining was performed on 4µm formalin fixed paraffin embedded sections (FFPE) heated at 60ºC for 2 hours.

The following antibodies were used to stain sections with a Leica Bond Rx autostainer: Cas9 (14697, Cell Signaling) and Ku80 (2180, Cell Signaling). All FFPE sections underwent on-board dewaxing (AR9222, Leica) and antigen retrieval using ER2 solution (AR9640, Leica) for 20 minutes at 95°C. Sections were rinsed with Leica wash buffer (AR9590, Leica) before peroxidase block was performed using an Intense R kit (DS9263, Leica) for 5 minutes. After rinsing with wash buffer, mouse Ig blocking solution (MKB-2213, Vector Labs) was applied to Cas9 sections for 20 minutes. Sections were rinsed with wash buffer and then primary antibody applied at an optimal dilution (Cas9, 1/250; Ku80, 1/400) for 30 minutes. The sections were rinsed with wash buffer and appropriate secondary antibody was applied for 30 minutes

(Cas9, Mouse Envision (Agilent, K4001); Ku80, Rabbit Envision (Agilent, K4003). The sections were rinsed with wash buffer and visualised using DAB with the Intense R kit.

Sections were stained for Ki67 Mib1 with an Agilent AutostainerLink48. These sections were loaded into an Agilent pre-treatment module to be dewaxed and undergo heat induced epitope retrieval (HIER, 97ºC for 20 minutes) using high pH target retrieval solution (TRS) (K8004, Agilent). After HIER sections were rinsed with flex wash buffer (K8007, Agilent) prior to being loaded onto the Agilent autostainer link48. The sections underwent peroxidase blocking (S2023, Agilent) for 5 minutes and rinsed with wash buffer. Sections had mouse Ig blocking reagent (MKB-2213, Vector Labs) applied for 20 minutes before rinsing with wash buffer. Ki67 primary antibody (M7240, Agilent) was applied at a 1/100 dilution for 30 minutes. Sections were rinsed with wash buffer before incubation with a mouse envision secondary antibody (K4001, Agilent) for 30 minutes. Sections were rinsed with wash buffer before applying Liquid DAB (K3468, Agilent) for 10 minutes. The sections were washed in water and counterstained with haematoxylin z (RBA-4201-00A, CellPath). To complete IHC staining FFPE sections were rinsed in tap water, dehydrated through graded ethanol's and placed in xylene. The stained sections were coverslipped in xylene using DPX mountant (SEA-1300-00A, CellPath). Slides were scanned at 20x magnification and analysed with HALO image analysis software (Indica labs).

Statistical analysis

Independent experimental replicate numbers and statistical tests are described in the figure legends. For all t-tests and ANOVA analyses, GraphPad Prism 9.0 or later versions were used. For the statistical analysis in figure 6F, we used the CGGC permutation test https://bioinf.wehi.edu.au/software/compareCurves/ to assess the significant differences between growth curves.

Results

Medium conditioned by breast cancer cells or cancer-associated fibroblasts increases colony formation efficiency of TNBC cells

Triple negative breast cancer (TNBC) cells' susceptibility to ferroptosis has been shown to be cell density dependent, with cells undergoing ferroptosis selectively when seeded at low density [16,23,24]. However, we have previously shown that TNBC cells seeded at low density are protected from ferroptosis by the sodium selenite present in the physiological cell culture medium Plasmax™ [16].

To dissect the mechanism underpinning the dependency of ferroptosis on culture density, we tested whether the anti-ferroptotic phenotype observed at high density was dependent on cell-cell interaction or transferrable with the conditioned medium. Medium conditioned for 48 hours by high-density cultures of MDA-MB-468 cells was employed to seed cells at low density, and it conferred the capacity to survive ferroptosis and form colonies comparably to cells supplemented with the anti-ferroptotic agent sodium selenite (**Figure 1A**). Similarly, medium conditioned by high-density cultures of human BT549, CAL-120, MDA-MB-231 and murine EO771 TNBC cells and employed to seed the respective cell lines at low density, significantly promoted colony formation (**Figure 1B**). This effect was not observed with the luminal A, ER-positive MCF7 breast cancer cells, for which the number of colonies was not altered by the conditioned medium.

Moreover, the medium conditioned by BT549, CAL-120 and MCF7 cells stimulated MDA-MB-468 colony-forming capacity, demonstrating that the anti-ferroptotic effect of conditioned medium is preserved across cell lines (**Figure 1C**). This observation prompted us to test if conditioned medium from untransformed cells could also support clonal growth of cancer cells. Cancer-associated fibroblasts (CAFs) are known to support the proliferation of cancer cells *in vivo* [20,25]. Conditioned medium from CAFs increased the colony formation capacity of MDA-MB-468 comparably to the anti-ferroptotic agent sodium selenite (**Figure 1D**). Conversely, neither the media conditioned by human normal fibroblasts from the mammary gland (MF), or from the dermis (DF), significantly increased the colony-forming capacity of MDA-MB-468 cells (**Figure 1D**). These data suggest that the medium conditioned by transformed or cancer-reprogrammed cells supports clonal growth of cancer cells by preventing ferroptosis.

Breast cancer cells cultured at high density produce and secrete an anti-ferroptotic factor

To test whether cells cultured at high density, condition the medium by depleting a ferroptosis inducing molecule (e.g. iron) or produce a factor that prevents ferroptosis, we collected

medium conditioned by high density MDA-MB-468 cells and diluted with fresh medium (1:3). The diluted conditioned medium enabled colony formation of MDA-MB-468 cells comparably to undiluted conditioned medium or sodium selenite supplementation (**Figure 2A**). These results suggest that breast cancer cells produce an anti-ferroptotic factor that compensates for the selenium deficiency. To identify this factor, we first fractionated the conditioned medium with a size exclusion column with a 10 kDa cut-off (**Figure 2B**). The flow-through fraction of the condition medium depleted of molecules > 10 kDa did not significantly increase the colony forming capacity of MDA-MB-468 cells compared to unconditioned medium. On the contrary the concentrated fraction of the conditioned medium enriched in molecules > 10 kDa significantly boosted the colony formation when used to supplement the fresh medium (**Figure 2C**). Moreover, its activity was retained when incubated for 15 min at 95ºC (**Figure 2D**). To further investigate the chemical properties of this factor we applied a Bligh and Dyer lipid extraction to the > 10kDa fraction of the condition medium. The extracted lipidic fraction used to supplement the medium of the MDA-MB-468 cells increased their colony forming capacity comparably to sodium selenite supplementation (**Figure 2E**). Altogether these results suggest that the anti-ferroptotic factor produced by TNBC cells at high density is a heat-resistant lipidic molecule bound to a carrier > 10 kDa.

Monounsaturated fatty acids prevent ferroptosis of TNBC cells

To gain an insight into the lipidic composition of the conditioned medium, we performed a lipidomic analysis on its fractions. Overall, we could detect 213 lipids from 12 classes, and all of them were more abundant in the > 10 kDa fraction (**Figure 3A**). Notably, 86% of the acyl chains of the detectable lipids had one (35%) or more double bonds (**Figure 3B**). In addition to the lipidic classes reported in Figure 3a, we could detect free C18:1 monounsaturated fatty acids (MUFA), that was also significantly more abundant in the > 10 kDa fraction (**Figure 3C**).

Based on this evidence, we tested if individual FA supplementation influenced the capacity of MDA-MB-468 cells to form colonies. At 50 µM, the saturated FA 16:0 and 18:0 did not have a significant effect on colony formation, while 7 out of the 8 MUFAs tested significantly increased the colony forming capacity (**Figure 3D**). Of the 7 MUFAs with colony stimulating activity, 4 (C16:1n7, C18:1n7, C18:1n9 and C20:1n9) retained their activity at 10 µM, a more physiological concentration (**Figure 3E**). In addition, 10 µM C18:1n9 (oleic acid) also increased the colony formation capacity in BT549 and CAL120 TNBC cells but not in MCF7 cells, thereby phenocopying the effects of conditioned medium on these breast cancer cell lines (**Figure 3F**).

SCD activity is required to condition the medium with an anti-ferroptotic factor

We noticed that all the MUFAs stimulating the clonogenic growth at 10 µM were products of the stearoyl-CoA desaturase (SCD), therefore we hypothesized that the presence of the anti-ferroptotic factor in the conditioned medium could be SCD-mediated. To test this, we conditioned medium employing MDA-MB-468 cells pre-treated with the SCD inhibitor CAY10566 or vehicle control and compared their colony-stimulating capacities (**Figure 4A**). SCD inhibition had no significant effects on the viability of high-density cultures employed to condition the medium (**Figure 4B**). Nevertheless, the medium conditioned by SCD-inhibited cells was significantly less effective in stimulating colony formation compared to medium conditioned by vehicle-treated cells (**Figure 4C**). Consistently with this observation, the levels of C16:1n7 (palmitoleic acid), a product of SCD, were significantly lower in the medium conditioned by SCD-pre-inhibited cells (**Figure 4D**).

To further validate these findings, we generated two SCD knockout (ko) clones derived from MDA-MB-468 cell lines (**Figure 4E**). Constitutive *SCD* deletion (SCDko) impaired cell proliferation in both clones (**Figure 4F**), therefore, to compensate for the lower number of cells during the conditioning of the medium, more SCDko cells than NTC cells were seeded (**Figure 4F**). Under these controlled culture conditions, the media from SCDko cells was significantly less potent in stimulating colony formation compared to medium conditioned by NTC cells (**Figure 4G**). These results indicate that SCD activity in TNBC cells is required to produce an anti-ferroptotic factor transferrable with the conditioned medium.

Cell density-dependent loss of SCD expression sensitizes TNBC cells to ferroptosis

After having demonstrated the anti-ferroptotic role of SCD-derived lipids in conditioned medium, we assessed whether SCD-deletion sensitizes TNBC cells to ferroptosis. We seeded NTC control MDA-MB-468 cells at a density at which their proliferation is maximal irrespective of sodium selenite and oleic acid supplementation (**Figure 5A**). At this cell density, the proliferation of both SCDko clones was significantly diminished, and partially rescued by the supplementation of oleic acid and sodium selenite. These results suggest that SCDko cells undergo ferroptotic cell death under these high-density conditions (**Figure 5A**). This notion was strengthened by the significant rescuing activity obtained with ferrostatin-1 in these conditions (**Figure 5B**). In addition, we treated NTC control and SCDko cells with 50 nM GPX4 inhibitor RSL3 (RAS-selective lethal) and observed ferroptotic cell death specifically in SCDko clones that was rescued by oleic acid supplementation (**Figure 5C**).

In line with the loss of SCD activity, we observed a significant decrease in the C16:1/C16:0 and C18:1/18:0 ratios in SCDko clones (**Figure 5D and E**). Unexpectedly, the levels of lipid peroxides were not significantly affected by *SCD* deletion (**Figure 5F**) suggesting that SCD-derived fatty acids desensitize cells from ferroptosis acting downstream of lipid peroxides.

To find a mechanistic rationale for the cell density-dependent susceptibility to ferroptosis observed in TNBC cells (i.e. maximal at low density), we assessed the levels of SCD expression and found that it was proportional to cell density in all four triple-negative breast cancer cell lines tested (**Figure 5G and H**). Consistently with the results shown in Figure 1B, the expression level of *SCD* was not modulated by cell density in the luminal A MCF7 cells (**Figure 5G**). Furthermore, the mRNA expression of key enzymes for fatty acid synthesis, elongation and desaturation (ACACA, FASN, ELOVL3, FADS1 and FADS2) was also downregulated at low cell density (**Figure 5I**).

These data showed that triple-negative breast cancer cells have an impaired fatty acid synthesis and desaturation capacity at low cell density thereby increasing their vulnerability to selenium starvation and ferroptosis.

Inhibition of selenocysteine synthesis induces ferroptosis and impairs lung metastatic colonization

GPX4 is a potent anti-ferroptotic enzyme whose catalytic activity requires selenocysteine in its active site. The amino acid selenocysteine is only synthesised on its tRNA and cannot be re-cycled as such for the synthesis of multiple selenoproteins (**Figure 6A**). This makes selenocysteine synthesis a limiting step to counteract ferroptosis and it could constitute a novel therapeutic target for ferroptosis-primed TNBC cells. On these bases, we designed guide RNAs (gRNAs) against three genes encoding enzymes of the synthesis pathway for selenocysteinilated $tRNA^{sec}$ (PSTK, SEPHS2 and SEPSECS, **Figure 6A**). The interference with the expression of each of the enzymes resulted in low GPX4 levels, comparable to those observed upon selenium starvation (**Figure 6B**). The loss of SEPHS2 expression or ferrostain-1 supplementation had no detrimental effects on the viability of cells seeded at high density, demonstrating that ferroptosis does not play a role under those conditions (**Figure 6C**). On the contrary, at low density cell survival depends on ferroptosis inhibition achieved by either selenium or ferroststatin-1 supplementation (see NTC Figure 6D). In these ferroptosis-priming conditions, the interference with SEPSECS, SEPHS2 and PSTK expression ablates the protective effect of selenium while Ferrostatin-1 retains its anti-ferroptotic effect. These results demonstrate that selenocysteine synthesis inhibition triggers ferroptosis selectively in isolated TNBC cells cultured at low density (**Figure 6D**).

Next, we orthotopically transplanted pools of NTC control and sgSEPHS2 MDA-MB-468 cells into the mouse mammary fat pad to investigate the effect of selenocysteine synthesis on tumour growth (**Figure 6 E-F**). The growth rate of sgSEPHS2 tumours was slower than NTC controls leading to a difference in tumour volume at endpoint that was confirmed by ex-vivo measurements (**Figure 6F-H**). In addition, the lower levels of SEPHS2 expression observed

in sgSEPHS2 pre-implantation (**Figure 6E**) were lost in tumours at endpoint (**Figure 6I**) suggesting that SEPHS2 expression is advantageous for tumorigenesis.

To assess whether the colonization of distant organs by TNBC cells is affected by selenocysteine synthesis inhibition, we injected luciferase-expressing NTC and sgSEPHS2 MDA-MB-468 cells into the tail vein of female NSG mice. Nine days after injection, the luciferase signal was detectable in the lungs of all mice, and it was significantly lower (~3-fold) in animals injected with sgSEPHS2 compared to NTC cells (**Figure 6J**). This difference was further exacerbated 36 days after injection (~5 fold) (**Figure 6K**). To validate the luciferase-based results, we stained the lungs of the tail vein-injected animals with antibodies against CAS9 and human Ku80 and Ki67 to detect individual metastatic cells (**Figure 6L**). We found seven times more Ki67- and Ku80-positive cells in lungs of mice injected with NTC cells (~0.4% of all cells in the lung) compared to sgSEPHS2 cells (~0.06%, **Figure 6M**). Notably, the ratio between Cas9- and Ku80-positive cells was significantly lower in mice injected with SEPHS2-depleted cells (**Figure 6N**) indicating that the expression of Cas9 is selectively lost in cells expressing sgSEPHS2. Overall, these *in vivo* results demonstrate that the expression of SEPHS2 is supporting the capacity of breast cancer cells to survive the bloodstream and colonize the lungs starting from single cells, recapitulating the requirement on selenocysteine synthesis for clonogenic growth observed *in vitro*.

Discussion

Understanding the regulation of ferroptotic cell death will provide new avenues to treat cardiovascular disease, neurodegenerative diseases, and cancer [26,27]. We and others have previously showed that selenium deprivation and inhibition of its uptake sensitizes to ferroptosis selectively when cells are at low density [16,17,24]. Here we demonstrate that in triple-negative breast cancer cells, the seeding density positively regulates the expression of genes involved in fatty acid synthesis and desaturation. Intriguingly, we found that medium conditioned by cancer cells and cancer associated fibroblasts cultured at high density has a pro-survival effect on cells seeded in colony forming assays (**Figure 1**). Specifically, we showed that the pro-clonogenic activity of the conditioned medium is thermostable and is retained in its lipidic fraction (**Figure 2E**). Moreover, the supplementation of specific monounsaturated fatty acids (MUFA) was effective in preventing ferroptosis occurring during colony formation (**Figure 3D**). Indeed, SCD-derived MUFAs are the most potent in rescuing ferroptosis when supplemented to cells at low density. Consistently, the loss of SCD activity in cells cultured at high density sensitises to ferroptosis (**Figure 5A-C**). These results suggest that diets low in SCD-derived MUFAs might enhance the efficacy of pro-ferroptotic agents such as SCD inhibitors [9]. In line with this hypothesis, Dierge et al showed that oleate-rich or PUFA-rich diets have opposite effects on the ferroptosis susceptibility of acidotic cancer cells, and Ubellacker et al described the anti-ferroptotic effects of oleic acid in melanoma [10,28]. We showed that unlike normal cells, high density cultures of cancer cells or cancer-associated fibroblasts secrete lipids containing monounsaturated fatty acid in the extracellular environment in quantities that prevent ferroptosis when supplemented to colony-forming cells (**Figure 1 and 2E**). Recently, it has been shown that primary breast tumours can secrete a factor that increases palmitate production in the lung, conditioning the metastatic niche to favour cancer cell growth [29]. Our results complement these findings and suggest that primary tumours, where cells are found at very high density, could secrete MUFA-containing lipids and alter the lipid composition in circulation thereby protecting metastasizing cells from ferroptosis. On these bases, we hypothesized that selenocysteine biosynthesis could be a novel target to clear ferroptosis-primed triple-negative breast cancer (TNBC) cells that have left the MUFA-rich environment of the primary tumour. Indeed, the interference with SEPHS2, an enzyme of the selenocysteine biosynthesis pathway (**Figure 6A**), decreases the growth of orthotopic primary tumours, and strongly impairs the seeding of cancer cells injected into the bloodstream in the lung (Figure 6F-N). In culture, we show that each of the three enzymes synthesizing the selenocysteinilated $tRNA^{sec}$ (PSTK, SEPHS2 and SEPSECS) as well as selenium supplementation are all required to prevent ferroptosis in cells seeded at low density (Figure 6). Carlisle et al have shown that high SEPHS2 expression correlates with poor survival in

patients with breast carcinoma and that its loss induces glioblastoma cell death by the accumulation of toxic H_2Se upon supraphysiological supplementation of sodium selenite [13]. Our data show that loss of SEPHS2 in TNBC cells phenocopies the cytotoxic effects of selenium deprivation and does not require the accumulation of toxic selenium metabolites to prime cells to ferroptosis (**Figure 6C-D**).

Breast cancer tissue shows increased level of protein-bound selenium compared to healthy tumour-surrounding tissue [30] suggesting an increased dependence on selenoprotein of cancer cells. While selenium-deprived diets have not been tested in breast cancer models, Eagle et al showed a therapeutic effect of selenium deprivation in leukaemia models while Alborzinia et al inhibited cellular selenoprotein P uptake to decrease the expression of selenoproteins and induce ferroptosis in neuroblastoma.

On the contrary, selenium-supplemented diets have been assessed with clinical trials (Select trial, NCT00006392) as preventive interventions for breast and prostate cancer with the rationale to boosts the antioxidant capacity of the host. However, whether diet intervention can lead to selenium concentrations that limit selenocysteine synthesis has yet to be established. Moreover, the pharmacologic inhibition of selenocysteinilated $tRNA^{sec}$ synthesis might have a more precise effect on the selenoprotein production in cancer cells that enter the blood circulation and depend on the antioxidant function of selenoproteins for their survival. Interestingly, PSTK shows low similarity to other eukaryotic kinases thereby favouring the design of specific small molecule inhibitors [31].

Taken together, our *in vitro* data show that SCD expression increases with cell density in TNBC cells and that its pharmacological inhibition abolishes the anti-ferroptotic capacity of medium conditioned by cells cultured at high density. Mechanistically, the SCD-dependent pro-survival effect is lost at low density when cells rely on the uptake of exogenous MUFAs and on the antioxidant action of selenoprotein to survive ferroptosis and form colonies. In vivo, we show that isolated TNBC cells injected in the bloodstream metastasize less efficiently to the lung when SEPHS2 activity is lost demonstrating that inhibition of the selenocysteinilated $tRNA^{sec}$ kills TNBC cells primed to ferroptosis by an imbalance in fatty acids saturation.

Acknowledgements: The authors thank the Core Services and Advanced Technologies at the Cancer Research UK Beatson Institute, and particularly the Metabolomics, Biological Services Unit, Histology Service and Molecular Technologies. The authors acknowledge Catherine Winchester for her comments on the manuscript, and all the members of the Oncometabolism lab for the constructive discussions. This work was funded by Cancer Research UK award A17196 and A31287 (CRUK Beatson Institute), Stand Up to Cancer campaign for CRUK grant A29800 (S.Z.), Breast Cancer Now 2018NovPR102 (S.Z.), Cancer Research UK award A29799 (K.B.) and Cancer Research UK award A23982 (S.T.).

Author contributions:

The study was conceptualized by T.A. and S.T.; methods were developed by E.S., G.R.B., C.N., V.H.V, D.S.; experiments were performed by T.A., E.S., R.D., J.A., L.C.A.G., B.A.S.; data were graphically visualized by T.A. and S.T.; the study was supervised by L.M. S.Z., K.B., D.S., S.T.; the manuscript was written by T.A. and S.T with reviewing and editing by all authors; funding was acquired by S.Z., K.B.,S.T..

Competing interests

All Authors declare no competing interests.

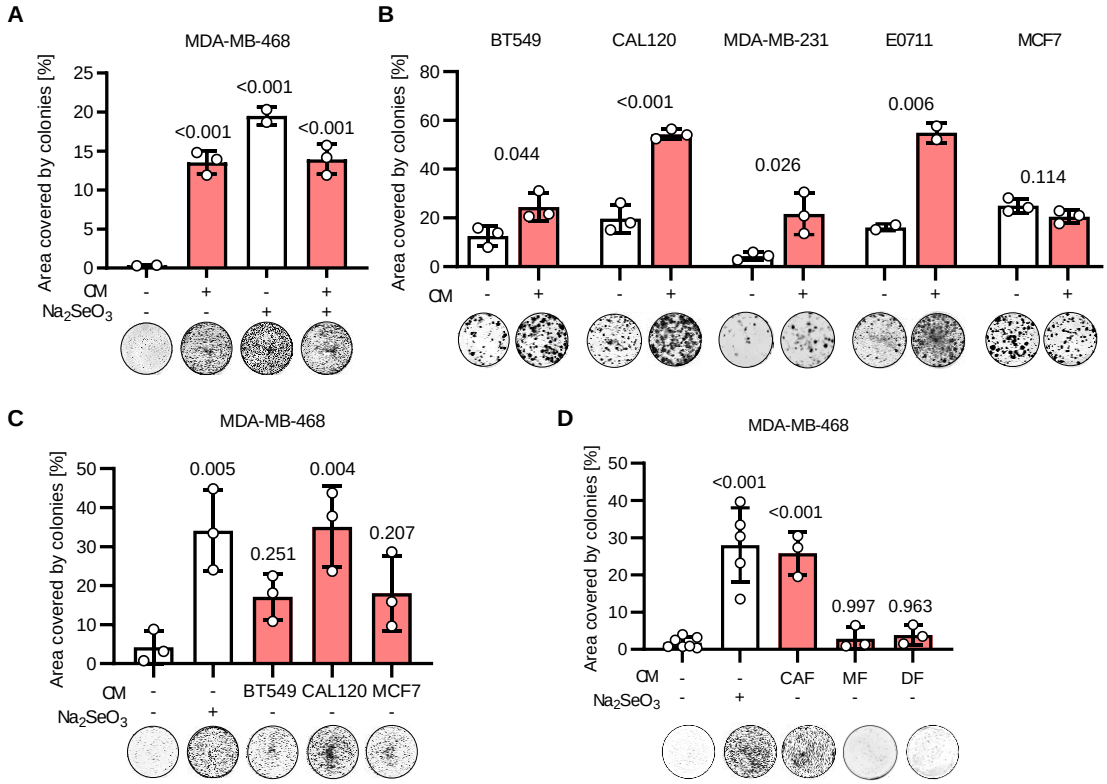

Figure 1: Medium conditioned by breast cancer cells and cancer-associated fibroblasts enhances the clonogenicity of triple-negative breast cancer cells.

A. Well area covered by colonies formed by MDA-MB-468 cells incubated for 7 days with mock medium or medium conditioned by MDA-MB-468 cells seeded at high density (CM). Media used for the colony forming assay were supplemented with 50 nM Na_2SeO_3 as indicated. P values refer to a two-way ANOVA test for unpaired samples with Dunnett's multiple comparisons test.

B. Well area covered by colonies formed by the indicated cell lines incubated for 7 days with mock medium or medium conditioned by BT549, CAL-120, MDA-MB-231, EO771 and MCF7 cells seeded at high density. Conditioned medium was used on the respective cell line. P values refer to a two-tailed, homoscedastic Student's *t* tests for unpaired samples.

C. Well area covered by colonies formed by MDA-MB-468 incubated for 7 days with mock medium or medium conditioned by BT549, CAL120 or MCF7 cells seeded at high density. Media used for the colony forming assay were supplemented with 50 nM Na_2SeO_3 as indicated. P values refer to a one-way ANOVA test for unpaired samples with Dunnett's multiple comparisons test.

D. Well area covered by colonies formed by MDA-MB-468 incubated for 7 days with mock medium or medium conditioned by cancer associated fibroblasts (CAF), immortalised mammary fibroblasts (MF), or immortalised human dermal fibroblasts (DF) seeded at high density. Media used for the colony forming assay were supplemented with 50 nM Na_2SeO_3 as

indicated. P values refer to a one-way ANOVA test for unpaired samples with Dunnett's multiple comparisons test.

A-D. Representative images of wells with colonies are shown for each experimental condition. n_{exp}=2-3 as indicated by the data points in each panel. Bars represent mean ± s.d..

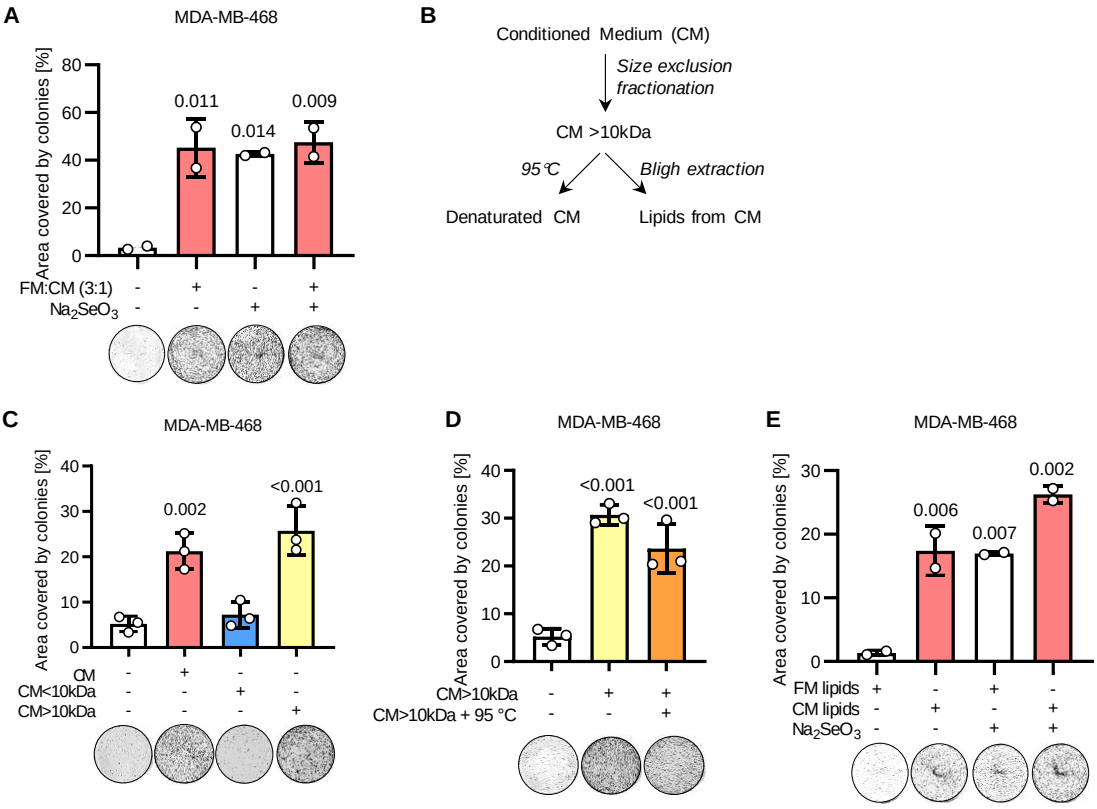

Figure 2: Breast cancer cells produce an anti-ferroptosis molecule at high density.

A. Well area covered by colonies formed by MDA-MB-468 incubated for 7 days with fresh medium (FM) or with FM mixed at the indicated ratio with medium conditioned by MDA-MB-468 cells seeded at high density (CM). P values refer to a two-way ANOVA test for unpaired samples with Dunnett's multiple comparisons test.

B. Schematic diagram of the analytical procedures applied to CM to identify the factor rescuing colony formation.

C-D. Well area covered by colonies formed by MDA-MB-468 incubated for 7 days with CM or with medium supplemented with the fractions separated by a size exclusion column as described in the Methods section (C) and further incubated for 15 min at 95°C (D). P values refer to a one-way ANOVA test for unpaired samples with Dunnett's multiple comparisons test.

E. Well area covered by colonies formed by MDA-MB-468 incubated for 7 days with fresh medium (FM) supplemented with lipidic extracts obtained as depicted in B. P values refer to a two-way ANOVA test for unpaired samples with Dunnett's multiple comparisons test.

A,C-E. Representative images of wells with colonies are shown for each experimental condition. n_{exp}=2-3 as indicated by the data points in each panel. Bars represent mean ± s.d..

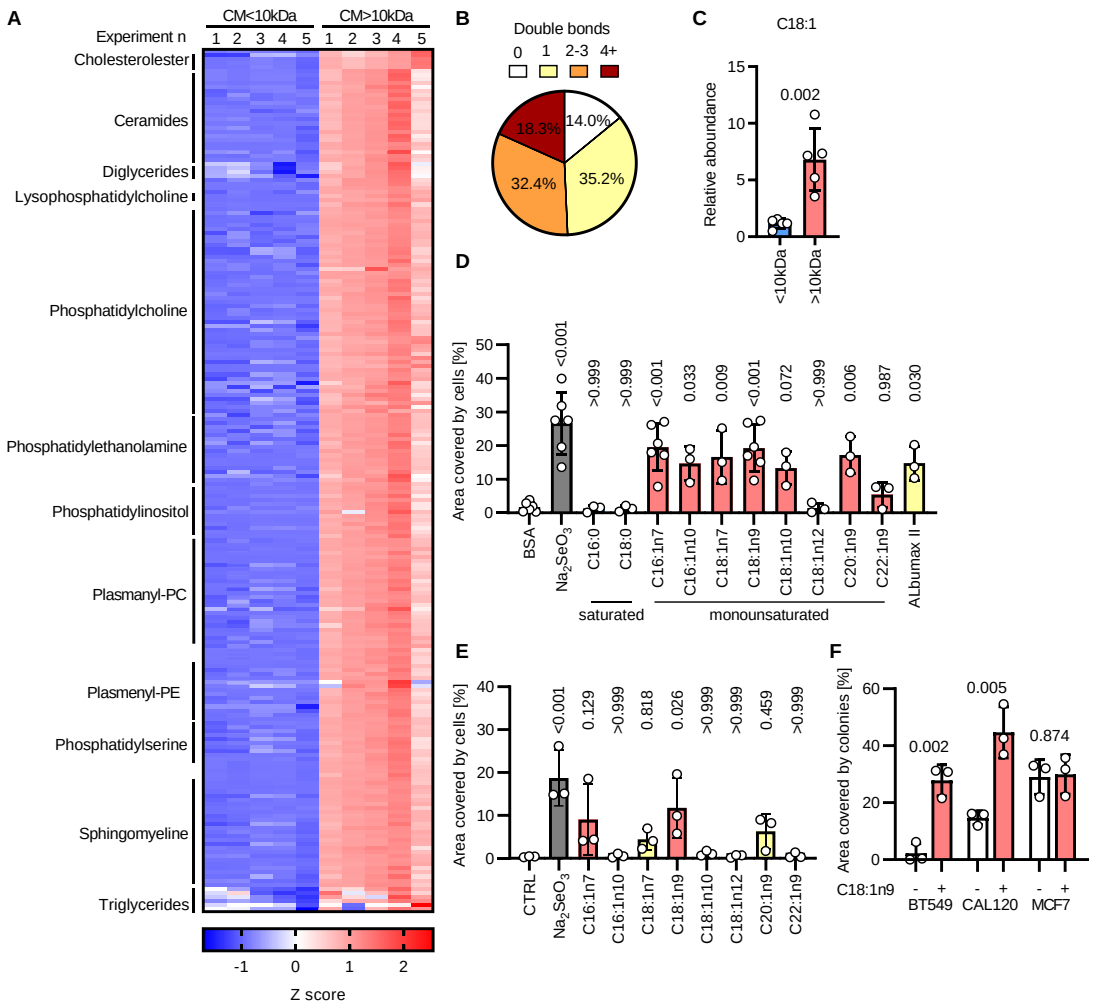

Figure 3: Monounsaturated fatty acids are enriched in the conditioned medium and prevent ferroptosis.

A. Heat map of lipids identified in medium conditioned and fractionated as described in Figure 2B-C. Selected classes of lipids are indicated. n_{exp}=5.

B. Pie chart depicting the fraction of lipid-bound fatty acids with 0, 1, 2-3, or ≥4 double bonds detected by LC-MS in the medium samples analysed in A.

C. Relative levels of C18:1 fatty acid identified in medium conditioned and fractionated as described in Figure 2B-C. Values are relative to the peak areas obtained in the <10 kDa fractions. P value refers to a two-tailed, homoscedastic Student's *t* tests for unpaired samples.

D. Well area covered by colonies formed by MDA-MB-468 cells incubated for 7 days with medium supplemented with 0.015% BSA, 0.015% BSA + 50 nM Na_2SeO_3 (Se), 0.015% BSA

+ 50 µM of the indicated fatty acids, lipid-rich BSA (Albumax II, 1.6g/L). P values refer to a one-way ANOVA test for unpaired samples with Dunnett's multiple comparisons test.

E. Well area covered by colonies formed by MDA-MB-468 cells incubated for 7 days with fresh medium (CTRL) or fresh medium supplemented with 50 nM Na_2SeO_3 (Se) or 10 µM of the indicated fatty acid. P values refer to a one-way ANOVA test for unpaired samples with Dunnett's multiple comparisons test.

F. Well area covered by colonies formed by the indicated cell lines incubated for 7 days with or without the supplementation of 10 µM oleic acid. P values refer to a two-tailed, homoscedastic Student's *t* tests for unpaired samples.

C-F. n_{exp}=3-5 as indicated by the data points. Bars represent mean ± s.d..

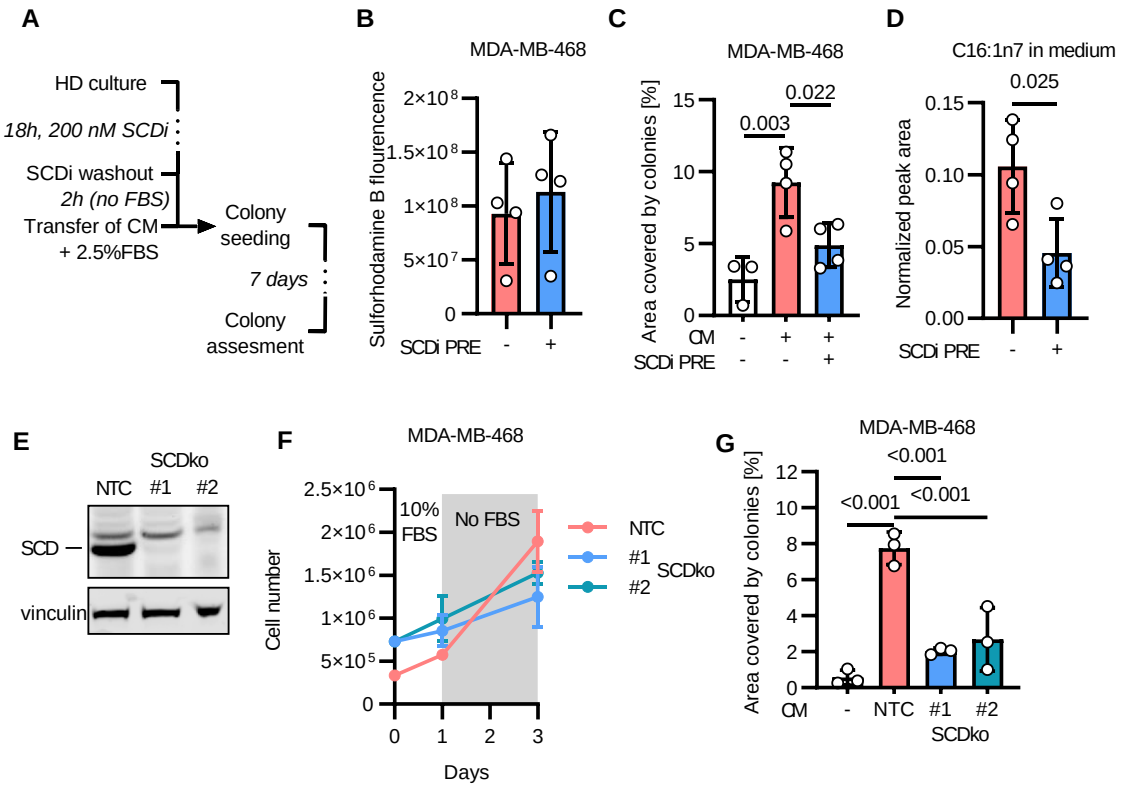

Figure 4: SCD is required for the anti-ferroptotic capacities of conditioned medium.

A. Schematic depicting the experimental workflow to condition the medium by MDA-MB-468 at high density (HD) pre-incubated with SCD inhibitor (CAY10566).

B. Quantification of Sulforhodamine B staining performed on MDA-MB-468 cells immediately after the conditioning of the medium with SCD inhibitor pre-treatment (SCDi PRE) as described in A.

C. Well area covered by colonies formed by MDA-MB-468 cells incubated for 7 days with mock medium and medium conditioned by MDA-MB-468 cells without or with SCD inhibitor pre-treatment (SCDi PRE). P values refer to a one-way ANOVA test for unpaired samples with Dunnett's multiple comparisons test.

D. Quantification of free and lipid-bound C16:1n7 level (palmitoleic acid) in medium conditioned by MDA-MB-468 cells without or with SCD inhibitor pre-treatment (SCDi PRE). Peak area values are normalized on the signal from internal standard (C17:0). P value refers to a two-tailed, homoscedastic Student's *t* tests for unpaired samples.

E. Immunoblot of SCD and vinculin in NTC and two SCDko clones from MDA-MB-468 breast cancer cells. Images representative of 3 independent experiments are shown.

F. Number of cells obtained with MDA-MB-468 NTC and SCDko clones cultured in conditions that recapitulate those used to condition the medium employed in G. n_{exp}=2

G. Well area covered by colonies formed by MDA-MB-468 cells incubated for 7 days with mock medium or medium conditioned by NTC or SCD ko MDA-MB-468 clones cultured as shown in F. P values refer to a one-way ANOVA test for unpaired samples with Dunnett's multiple comparisons test.

B-D, G. n_{exp}=2-4 as indicated by the data points in each panel. Bars represent mean ± s.d..

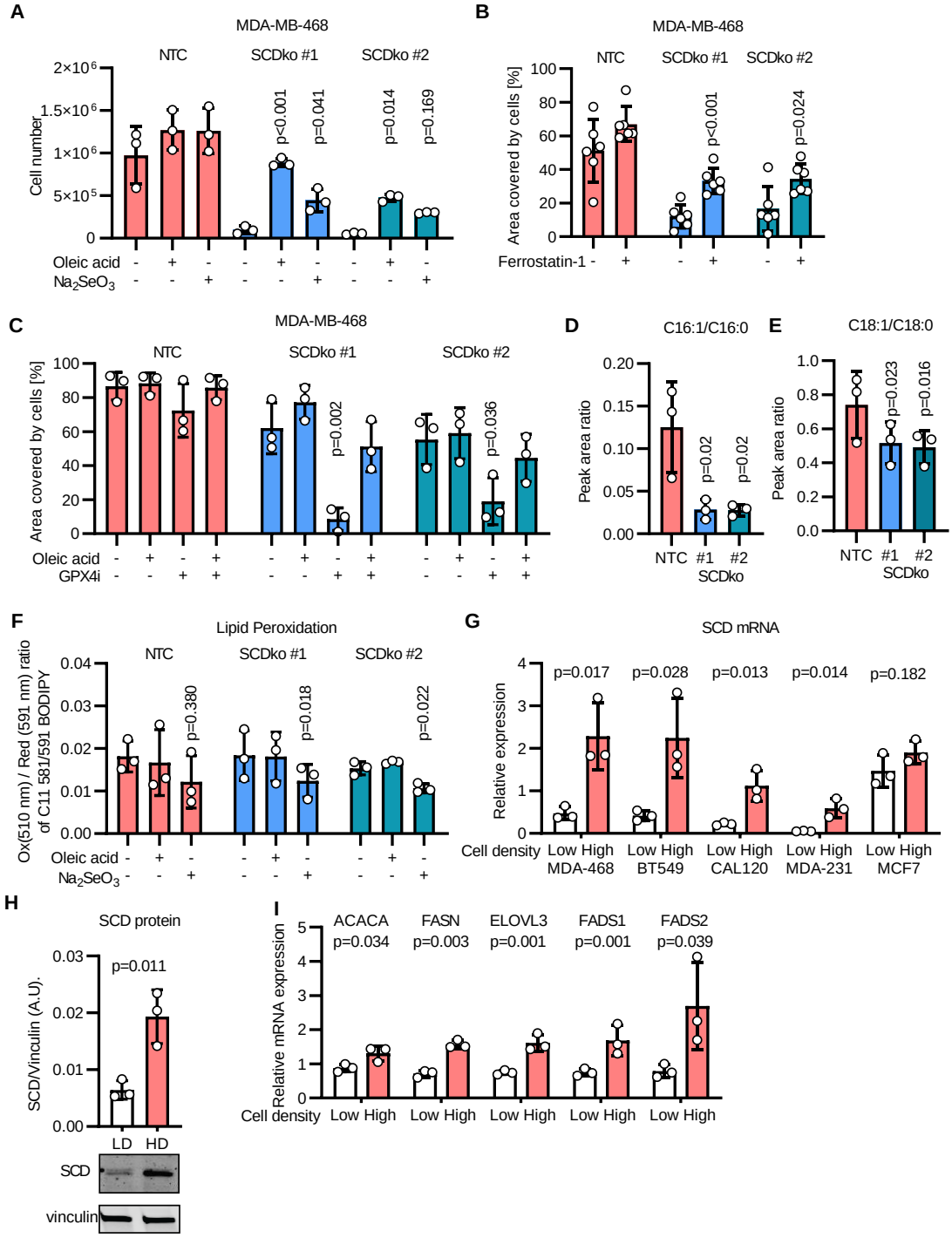

Figure 5: Loss of SCD sensitises cells to ferroptosis.

A. Number of NTC and SCDko MDA-MB-468 cells seeded at high density and incubated for 5 days without or with 10 µM oleic acid or 50 nM Na_2SeO_3 as indicated. P values refer to a two-way ANOVA test for unpaired samples with Dunnett's multiple comparisons test.

B. Well area covered by NTC and SCDko MDA-MB-468 cells seeded at high density and incubated for 5 days without or with 1 µM ferrostatin-1. P values refer to a two-tailed, homoscedastic Student's *t* tests for unpaired samples.

C. Well area covered by NTC and SCDko MDA-MB-468 cells seeded at high density and incubated for 5 days without or with 50 nM GPX4 inhibitor (RSL3), 10 µM Oleic acid or their combination (50 nM and 10 µM respectively). P values refer to a two-way ANOVA test for unpaired samples with Dunnett's multiple comparisons test.

D-E. Ratio of C16:1 / C16:0 (D) and C18:1 / C18:0 (E) fatty acids in NTC and SCDko MDA-MB-468 cells seeded at high density. P values refer to a one-way repeated measures repeated measures ANOVA test for paired samples with Dunnett's multiple comparisons test.

F. Ratio between oxidised (510 nm) and reduced (591 nm) BODIPY 581/591 C11 (lipid peroxidation sensor) in NTC and SCDko MDA-MB-468 cells seeded at high density and incubated for 2 days without or with 10 µM oleic acid or 50 nM Na_2SeO_3. P values refer to a one-way repeated measures ANOVA test for paired samples with Dunnett's multiple comparisons test.

G. qPCR quantification of *SCD* mRNA expression in MDA-MB-468, BT549, CAL120, MDA-MB-231 and MCF7 cells seeded at low and high density and cultured for 2 days. The expression is relative to Actin mRNA abundance. P values refer to a two-tailed, homoscedastic Student's *t* tests for unpaired samples.

H. Immunoblot analysis of SCD level in MDA-MB-468 cells seeded at low and high density and cultured for 2 days. A representative image of SCD and vinculin from one of the 3 experiments quantified in the upper panel. P value refers to a two-tailed, homoscedastic Student's *t* tests for unpaired samples.

I. qPCR quantification of *ACACA, FASN, ELOVL3, FADS1* and *FADS2* mRNA expression in MDA-MB-468 cells seeded at low and high density and cultured for 2 days. The expression is relative to Actin mRNA abundance. P values refer to a two-tailed, homoscedastic Student's *t* tests for unpaired samples.

A-I. n_{exp}=3-6 as indicated by the data points in each panel. Bars represent mean ± s.d..

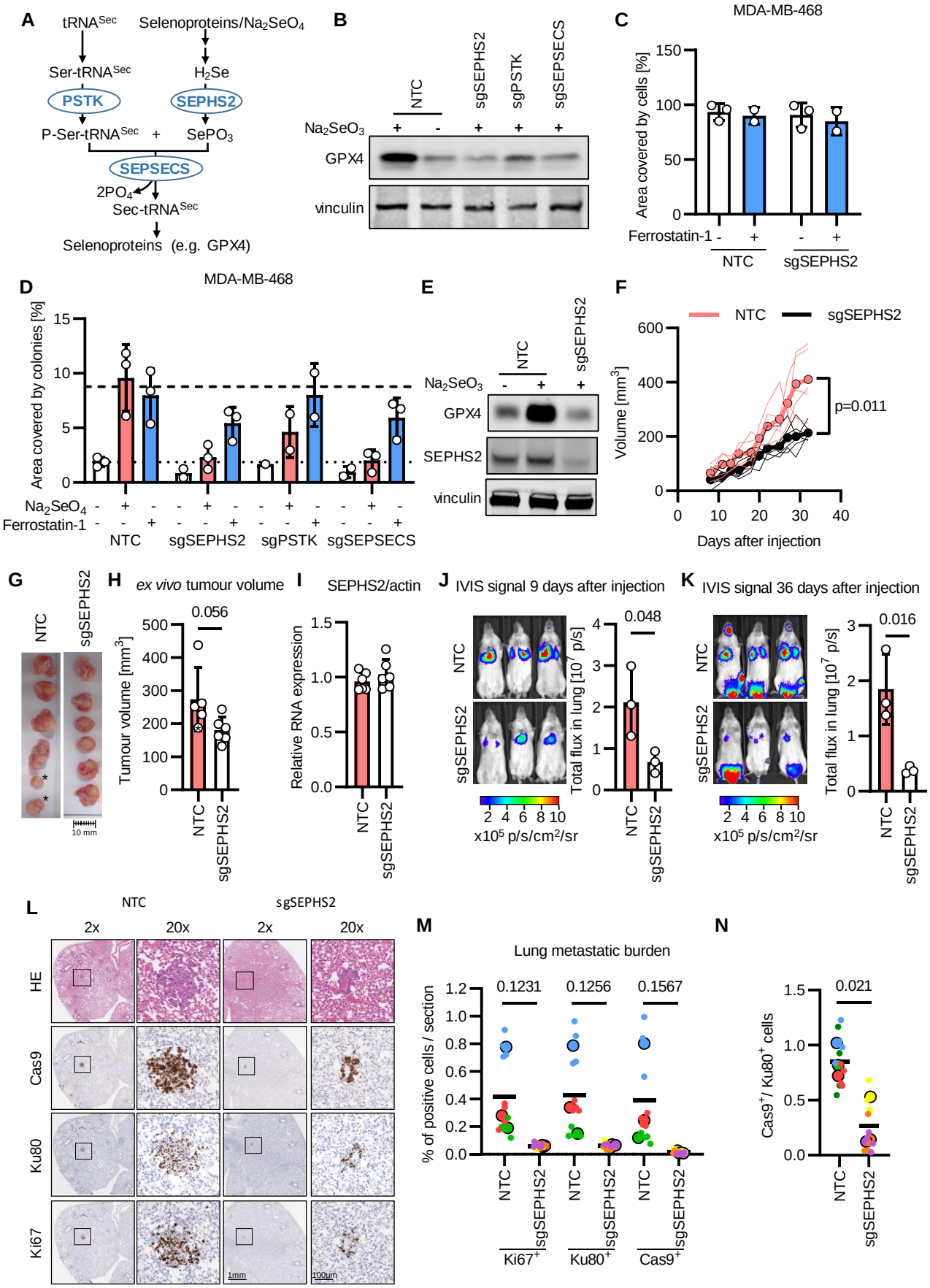

Figure 6: Targeting selenocysteine biosynthesis impairs lung metastatization of TNBC.

A. Schematic depicting selenocysteine synthesis on $tRNA^{sec}$.

B. Immunoblot images of GPX4 and vinculin in control MDA-MB-468 cells (NTC) or in cells depleted of PSTK, SEPHS2 and SEPSECS supplemented with 50 nM Na_2SeO_3 as indicated.

C. Well area covered by NTC and sgSEPHS2 MDA-MB-468 cells seeded at high density and incubated for 5 days without or with 1 µM ferrostatin-1. n_{exp}=2-3 as indicated by the data points. Bars represent mean ± s.d..

D. Well area covered by colonies formed by NTC, sgSEPHS2, sgPSTK and sgSEPSECS MDA-MB-468 cells seeded at low density and incubated for 7 days without and with 50 nM Na_2SeO_3 or 1 µM ferrostatin-1. n_{exp}=1-3 as indicated by the data points. Bars represent mean ± s.d..

E. Immunoblot images of GPX4, SEPHS2 and vinculin in MDA-MB-468 cells (NTC) or in cells depleted of SEPHS2 supplemented with 50 nM Na_2SeO_3 as indicated. Images representative of 3 independent experiments.

F. Calliper-measured volume of tumours in the mammary fat pad of female NSG mice injected with NTC (n=3) or sgSEPHS2 (n=3) MDA-MB-468 cells. All mice were injected bilaterally with $3x10^6$ cells with the exception of one mouse in the NTC group that received only one injection due to a technical issue. When multiple tumours were formed from a single injection of cells (as indicated in G) their combined volumes were reported as one data point. Thinner lines represent the volumes of tumours obtained from each fat pad injection, thicker lines and symbols represent group means (n=5 tumours for NTC and n= 6 for sgSEPHS2). A CGGC permutation test (https://bioinf.wehi.edu.au/software/compareCurves/) was used to assess the significant differences between growth curves. P value refers to a test with 1000 permutations.

G. Pictures of NTC or sgSEPHS2 MDA-MB-468 resected tumours taken *ex vivo* 35 days after injections. * Indicates two tumours in the same mammary fat pad derived from a single injection.

H. E*x vivo* quantification of the volume of tumours shown in G. The volumes of tumours indicated with * in G are summed and reported as one data point indicated with a *. P values refer to a two-tailed, homoscedastic Student's *t* tests for unpaired samples. n=5-6 tumours as indicated by the data points.

I. qPCR quantification of *SEPHS2* mRNA expression in the tumours shown in G. The expression is relative to Actin mRNA abundance. n=5-6 tumours as indicated by the data points.

J-K. IVIS pictures and quantification of lung metastasis burden 9 days (J) and 36 days (K) after tail vein injection of $2x10^6$ NTC or sgSEPHS2 MDA-MB468 cells. P value refers to a two-tailed, homoscedastic Student's *t* tests for unpaired samples. n=3 female NSG mice.

L. Representative images of staining with haematoxylin and eosin (HE), human Ki67, human Ku80 and Cas9 of lungs of mice described in J-K seven weeks after tail vein injection. Black squares frame the areas magnified at 20x.

M. Lung metastasis burden assessed by quantifying the % of human Ki67, human Ku80 and Cas9 positive cells in lungs of mice described in J-K seven weeks after tail vein injection. P values refer to a two-tailed, homoscedastic Student's *t* tests for unpaired samples.

N. Ratio between Cas9 and hKu80 positive cells in lungs of mice described in J-K seven weeks after tail vein injection. P value refers to a two-tailed, homoscedastic Student's *t* tests for unpaired samples.

M-N Large circles represent data points that are calculated as mean of four replicate sections indicated by smaller circles. Colours of data points indicate individual animals. Lines represent group means (n=3 mice).

References

1. Yang, W. S. & Stockwell, B. R. Ferroptosis : Death by Lipid Peroxidation. *Trends Cell Biol* **26**, 165–176 (2016).
2. Zheng, J. & Conrad, M. The Metabolic Underpinnings of Ferroptosis. *Cell Metab* **32**, 920–937 (2020).
3. Bersuker, K. *et al.* The CoQ oxidoreductase FSP1 acts parallel to GPX4 to inhibit ferroptosis. *Nature* **575**, (2019).
4. Mishima, E. *et al.* A non-canonical vitamin K cycle is a potent ferroptosis suppressor. *Nature* **608**, (2022).
5. Yang, W. S. *et al.* Regulation of Ferroptotic Cancer Cell Death by GPX4. *Cell* **156**, 317–331 (2014).
6. Doll, S. *et al.* ACSL4 dictates ferroptosis sensitivity by shaping cellular lipid composition. *Nat Chem Biol* **13**, 91–98 (2017).
7. Song, X. *et al.* PDK4 dictates metabolic resistance to ferroptosis by suppressing pyruvate oxidation and fatty acid synthesis. *Cell Rep* **34**, 108767 (2021).
8. Magtanong, L. *et al.* Exogenous Monounsaturated Fatty Acids Promote a Ferroptosis-Resistant Cell State. *Cell Chem Biol* **26**, 420-432.e9 (2019).
9. Tesfay, L. *et al.* Stearoyl-CoA desaturase 1 protects ovarian cancer cells from ferroptotic cell death. *Cancer Res* **79**, 5355–5366 (2019).
10. Ubellacker, J. M. *et al.* Lymph protects metastasizing melanoma cells from ferroptosis. *Nature* **585**, 113–118 (2020).
11. Labunskyy, V. M., Hatfield, D. L. & Gladyshev, V. N. Selenoproteins: Molecular Pathways and Physiological Roles. *Physiol Rev* **94**, 739–777 (2014).
12. Burk, R. F. & Hill, K. E. Regulation of Selenium Metabolism and Transport. (2015) doi:10.1146/annurev-nutr-071714-034250.
13. Carlisle, A. E. *et al.* Selenium detoxification is required for cancer-cell survival. *Nat Metab* **2**, 603–611 (2020).
14. Chen, Y.-C., Prabhu, K. S. & Mastro, A. M. Is Selenium a Potential Treatment for Cancer Metastasis? *Nutrients* **5**, 1149–1168 (2013).
15. Eagle, K. *et al.* An oncogenic enhancer encodes selective selenium dependency in AML. *Cell Stem Cell* **29**, 386-399.e7 (2022).
16. vande Voorde, J. *et al.* Improving the metabolic fidelity of cancer models with a physiological cell culture medium. *Sci Adv* **5**, eaau7314 (2019).
17. Alborzinia, H. *et al.* Selenocysteine metabolism is a targetable vulnerability in MYCN-amplified cancers 1 2. doi:10.1101/2022.05.17.492172.
18. Vinceti, M. *et al.* Selenium for preventing cancer. *Cochrane Database of Systematic Reviews* vol. 2014 Preprint at https://doi.org/10.1002/14651858.CD005195.pub3 (2014).

19. National Institutes of Health - Office of Dietary Supplements. Selenium - Fact Sheet for Health Professionals. *https://ods.od.nih.gov/factsheets/Selenium-HealthProfessional/* (2023).

20. Kojima, Y. *et al.* Autocrine TGF-β and stromal cell-derived factor-1 (SDF-1) signaling drives the evolution of tumor-promoting mammary stromal myofibroblasts. *Proc Natl Acad Sci U S A* **107**, 20009–20014 (2010).

21. Hernandez-Fernaud, J. R. *et al.* Secreted CLIC3 drives cancer progression through its glutathione-dependent oxidoreductase activity. *Nat Commun* **8**, (2017).

22. Hutchins, P. D., Russell, J. D. & Coon, J. J. LipiDex: An Integrated Software Package for High-Confidence Lipid Identification. *Cell Syst* **6**, 621-625.e5 (2018).

23. Panzilius, E. *et al.* Cell density-dependent ferroptosis in breast cancer is induced by accumulation of polyunsaturated fatty acid-enriched triacylglycerides. *bioRxiv* (2018) doi:10.1101/417949.

24. Wu, J. *et al.* Intercellular interaction dictates cancer cell ferroptosis via NF2–YAP signalling. *Nature* **572**, 402–406 (2019).

25. Sahai, E. *et al.* A framework for advancing our understanding of cancer-associated fibroblasts. *Nature Reviews Cancer* vol. 20 174–186 Preprint at https://doi.org/10.1038/s41568-019-0238-1 (2020).

26. Chen, Z. *et al.* The Role of Ferroptosis in Cardiovascular Disease and Its Therapeutic Significance. *Front Cardiovasc Med* **8**, 733229 (2021).

27. Yan, H. fa *et al.* Ferroptosis: mechanisms and links with diseases. *Signal Transduction and Targeted Therapy* vol. 6 Preprint at https://doi.org/10.1038/s41392-020-00428-9 (2021).

28. Dierge, E. *et al.* Peroxidation of n-3 and n-6 polyunsaturated fatty acids in the acidic tumor environment leads to ferroptosis-mediated anticancer effects. *Cell Metab* **33**, 1701-1715.e5 (2021).

29. Altea-Manzano, P. *et al.* A palmitate-rich metastatic niche enables metastasis growth via p65 acetylation resulting in pro-metastatic NF-κB signaling. *Nat Cancer* (2023) doi:10.1038/s43018-023-00513-2.

30. Charalabopoulos, K. *et al.* Selenium in serum and neoplastic tissue in breast cancer: correlation with CEA. *Br J Cancer* **95**, 674–676 (2006).

31. Sherrer, R. L., O'Donoghue, P. & Söll, D. Characterization and evolutionary history of an archaeal kinase involved in selenocysteinyl-tRNA formation. *Nucleic Acids Res* **36**, 1247–1259 (2008).